

# Catalytic Pyrolysis of Tar Model Compound with Various Bio-Char Catalysts to Recycle Char from Biomass Pyrolysis

Jinmiao Liu,<sup>a</sup> Yanfeng He,<sup>a,\*</sup> Xinxin Ma,<sup>a</sup> Guangqing Liu,<sup>a</sup> Yao Yao,<sup>a</sup> Hui Liu,<sup>a</sup> Hong Chen,<sup>a</sup> Yan Huang,<sup>a</sup> Chang Chen,<sup>b</sup> and Wen Wang<sup>a</sup>

Tar and char can be regarded as unwanted byproducts during the gasification process. In this study, three types of catalyst, *i.e.*, biomass char (bio-char), nickel supported on biomass (Ni+bio-char), and nickel supported on bio-char (bio-char+Ni), were studied to compare the catalytic effects of different preparation methods on tar model compound removal. The structural characteristics of the three catalysts were also investigated by X-ray diffraction (XRD), scanning electron microscopy (SEM), and Brunauer-Emmett-Teller (BET) methods. The results revealed that Ni+bio-char catalyst showed much higher activity for the reformation of toluene (C<sub>7</sub>H<sub>8</sub>) as a tar model compound than the other two catalysts. Toluene could be completely converted to small gas molecules at a conversion rate of 99.92% at 800 °C, and the maximum yield of gas was 432 mL/(mL C<sub>7</sub>H<sub>8</sub>). In particular, the H<sub>2</sub> and CH<sub>4</sub> yields were 339 and 85 mL/(mL C<sub>7</sub>H<sub>8</sub>) at 850 °C, respectively. An N<sub>2</sub> absorption-desorption experiment demonstrated that the specific surface area of Ni+bio-char was 32.87 times that of bio-char and 8.39 times that of bio-char+Ni. Moreover, metallic nickel (Ni<sup>0</sup>) particles could be generated in the carbon matrix of Ni+bio-char catalyst. SEM analysis confirmed that the Ni+bio-char catalyst had a more porous structure. Nickel supported on biomass might be a promising catalyst for tar reformation because of its excellent catalytic activities.

*Keywords:* Bio-char; Char-supported catalyst; Tar reformation; Catalytic pyrolysis; Metal impregnation

*Contact information:* a: Biomass Energy and Environmental Engineering Research Center, College of Chemical Engineering, Beijing University of Chemical Technology, Beijing 100029, China; b: College of Life Science and Technology, Beijing University of Chemical Technology, Beijing 100029, China;

\* Corresponding author: litasha@126.com

## INTRODUCTION

Because of the shortage of fossil fuel reserves and environmental concerns, along with the high energy demand in the world, the utilization of biomass has attracted increasing attention as an alternative energy resource. Biomass gasification is considered to be the core and the promising option among many low-pollution emission technologies to transform biomass into syngas (Li and Suzuki 2009; Min *et al.* 2011a). The produced syngas can be used directly for power generation or catalytically converted to methanol, liquid hydrocarbons *via* Fischer-Tropsch synthesis, and other chemical products (Han and Kim 2008). However, the presence of tar in biomass gasification is a critical problem because it can cause many difficulties for the operation of downstream applications associated with condensation, blockage, corrosion, and even polymerization to form more complex structures in pipes. Moreover, the existence of tar may pose environmental

hazards and potential health problems because many components of tar may be carcinogenic or mutagenic. Therefore, tar reduction is one of the most challenging barriers to the development of biomass gasification technology.

There are several approaches to tar reformation, such as physical methods, thermal cracking, and catalytic reformation (Wang *et al.* 2010). Liquid scrubbing is one of the physical methods and usually produces a large amount of wastewater containing high amounts of aromatics, leading to the loss of total thermal efficiency. Thermal cracking is not practically feasible because it requires an operating temperature above 1100 °C to realize effective tar decomposition. Catalytic pyrolysis can reduce tar generation, but in many cases, as the reaction proceeds, the catalyst will deactivate because of carbon deposition and particle agglomeration, resulting in reduced pyrolysis efficiency and requiring regular catalyst replacement. Therefore, some authors have proposed an innovative approach to insert the catalyst inside the substrate before the thermo-chemical conversion. Using this method, catalytic material can be dispersed in the matrix and freshly renewed when it is introduced into the reactor, thus avoiding the problems that have been encountered with conventional catalytic methods.

Nickel is considered to be an excellent element for tar removal because of its catalytic activity and economic factors. Ni-Al<sub>2</sub>O<sub>3</sub>/MgO (Sato and Fujimoto 2007; Yue *et al.* 2010) or Ni supported by natural materials (*e.g.*, dolomite, ilmenite) (Le *et al.* 2009; Lee and Ihm 2009) are commonly used as catalysts. However, the catalyst preparation process is complex and accompanied by energy consumption; thus, the catalyst is relatively expensive (Li and Suzuki 2009; Yung *et al.* 2009; Xu *et al.* 2010). To improve the catalytic performance of nickel catalysts in the removal of tar, several solutions have been employed, such as changing the support and/or adding promoters.

Bio-char is employed as a good catalyst or catalyst support candidate because of its highly porous structures. Wang *et al.* (2011) studied the catalytic performance of Ni/char catalysts by mechanically mixing NiO and char particles. It was found that the tar removal rate was more than 97% in syngas with Ni/char catalysts under the reforming conditions of 800 °C reforming temperature, 15% NiO loading, and 0.3 s gas residence time. Shen *et al.* (2014) found that the *in-situ* tar conversion efficiency could reach approximately 92.3% at 800 °C using rice husk char supported Ni-Fe catalysts, which exhibited advantages of easy preparation and energy savings. Min *et al.* (2011b) reported that char-supported iron/nickel catalysts have higher activity than char itself because char can disperse the catalysts and interact with the catalysts in the process of tar reformation.

There are three types of methods to prepare char-supported catalysts. Char-supported catalyst (1) is made by mechanically mixing metal ions with bio-char, which can cause metal particles to stay only on the outer surface of the char support. Char-supported catalyst (2) is made by pyrolysis of metal ion-impregnated biomass. Finally, char-supported catalyst (3) is made by impregnating bio-char. The latter two catalysts are better than catalyst (1) because impregnation can easily disperse metal inside the solid fuel, as suggested by our previous study (Zhang *et al.* 2013a). Char-supported catalyst (2) is considered to be more efficient than the other two catalysts for tar reformation because metal with nanoparticles could also be formed inside the support *via* the impregnation and pyrolysis. However, there has been little research on that aspect up to the present.

Numerous studies have reported that metals remain in char after pyrolysis of metal-impregnated biomass; therefore, pyrolysis of metal-impregnated biomass can produce chars enriched with metal nanoparticles, *e.g.*, Ni<sup>0</sup> NPs, which can be used as a promising candidate for the follow-up tar reformation process (Wang *et al.* 2011; Zhang *et al.*

2013b,c). Tar and char are always unwanted byproducts during the gasification process; therefore, an appropriate method is needed to effectively transform them. By using impregnation catalytic technology, one can build an integrated biomass pyrolysis/gasification system to process tar and char simultaneously. The process includes the following: (1) using an impregnation method to insert metal precursor into the biomass matrix, (2) catalytic pyrolysis of biomass to generate metal-impregnated bio-char, (3) *in-situ* catalytic conversion of original tar over the freshly formed metal-impregnated bio-char, (4) catalytic gasification of the char residue, and (5) recycling and reuse of the catalyst metal species in the ashes. Among these steps, there has been a lack of studies on step (3); therefore, it is of vital significance in the research on catalytic activities of char-supported catalysts and the functions of char during the tar reformation process.

To elucidate tar reformation during the gasification process, many researchers have utilized aromatics as tar model compounds to investigate the decomposition behavior; these include phenol (Park *et al.* 2010), naphthalene (Furusawa and Tsutsumi 2005), and toluene (Swierczynski *et al.* 2008; Zhao *et al.* 2010). Most studies have used toluene as a model compound because it is an important aromatic compound and represents the stability of the aromatic structure in tar formed with a high-temperature process (Kong *et al.* 2011). Therefore, for a better understanding of tar removal, toluene was chosen as a model compound in this study. The objectives of this research were to (1) examine the feasibility of using char or char-supported catalysts in gasification processes, (2) compare the catalytic effects of different catalysts on tar model compound removal, and (3) investigate the structural characteristics of three catalysts by scanning electron microscopy (SEM), X-ray diffraction (XRD), and Brunauer-Emmett-Teller (BET) methods.

## EXPERIMENTAL

### Materials

Poplar wood obtained from Henan province, China, was used as the raw material to prepare the char and Ni-impregnated char. The air-dried poplar wood was chopped and then pulverized to particle sizes between 1 and 5 mm using a laboratory ball-miller. The samples were stored in airtight plastic bags at room temperature for further use. The proximate analysis of the samples was determined according to standard methods (Donahue and Rais 2009). Elemental compositions (C, H, N, S) were determined using an elemental analyzer (Vario Elcube, Germany). Element 'O' was estimated by difference. The analytical properties of the samples are listed in Table 1.

**Table 1.** Proximate and Ultimate Analysis

Sample	Proximate analysis (wt%)			Ultimate analysis (wt%)				
	Ash <sup>a</sup>	Volatile matter <sup>b</sup>	Fixed Carbon <sup>b</sup>	C <sup>b</sup>	H <sup>b</sup>	O <sup>b,c</sup>	N <sup>b</sup>	S <sup>b</sup>
Poplar wood	2.96	85.36	14.64	47.64	6.26	45.69	0.31	0.10
Impregnated-wood	10.63	86.08	13.92	69.89	0.57	28.46	0.96	0.12
Bio-char	5.31	7.22	92.78	88.69	1.12	9.53	0.47	0.19
Ni+bio-char	35.22	11.08	88.93	38.55	4.75	54.71	1.96	0.03
Bio-char+Ni	9.49	31.65	68.36	75.14	1.17	21.63	2.00	0.06

<sup>a</sup> Dry basis; <sup>b</sup> Dry and ash-free basis; <sup>c</sup> By difference

## Catalyst Preparation

Three types of catalysts were prepared in this work: biomass char, char of nickel-impregnated biomass, and nickel supported on bio-char (Table 1). The biomass char catalyst, denoted as “bio-char,” was prepared at atmospheric pressure in a fixed-bed pyrolysis reactor. First, approximately 60 g of poplar wood particles of 1 to 5 mm were fed into the reactor, which was heated to 850 °C at a heating rate of 20 °C /min with continuous argon flow. At 850 °C, the poplar wood particles were pyrolyzed for 90 min. Finally, the char samples were collected after the reactor was lifted out of the furnace and cooled to room temperature. The method to prepare char of nickel-impregnated biomass, denoted as “Ni+bio-char,” was the same as that of bio-char except that the poplar wood particles were impregnated beforehand with a 0.5 M Ni(NO<sub>3</sub>)<sub>2</sub> solution for three days in the shaking-table. After impregnation, the samples were then filtered and washed with impregnation liquid to remove the metal ions that did not combine with the material. Finally, the impregnated samples were pyrolyzed in a fixed-bed reactor after being dried at 105 °C overnight. The nickel supported on bio-char, denoted “bio-char+Ni,” was obtained by impregnating the biomass char in a 0.5 M Ni(NO<sub>3</sub>)<sub>2</sub> solution for three days in the shaking-table, washing, and drying at 105 °C overnight. The three types of catalysts were collected and sieved into particle sizes of 0.45 to 0.90 mm for subsequent use. Because the impregnation method can generate large of wastewater / impregnation solution, we will study the possible of impregnating samples by recycling impregnation solution in future work.

## Reformation of Toluene

The reformation of toluene was performed in a two-stage fixed-bed stainless steel reactor, the stages of which are denoted as the gasification reactor and the catalytic reforming reactor (Fig. 1). The two-stage reactor was independent, and both of them heated with an electric furnace to maintain different temperatures during the reformation experiment. Each reactor was 18.4 mm in diameter and 60 mm in length. Two thermocouples were inserted into the reactors to measure the temperature of the two stages.

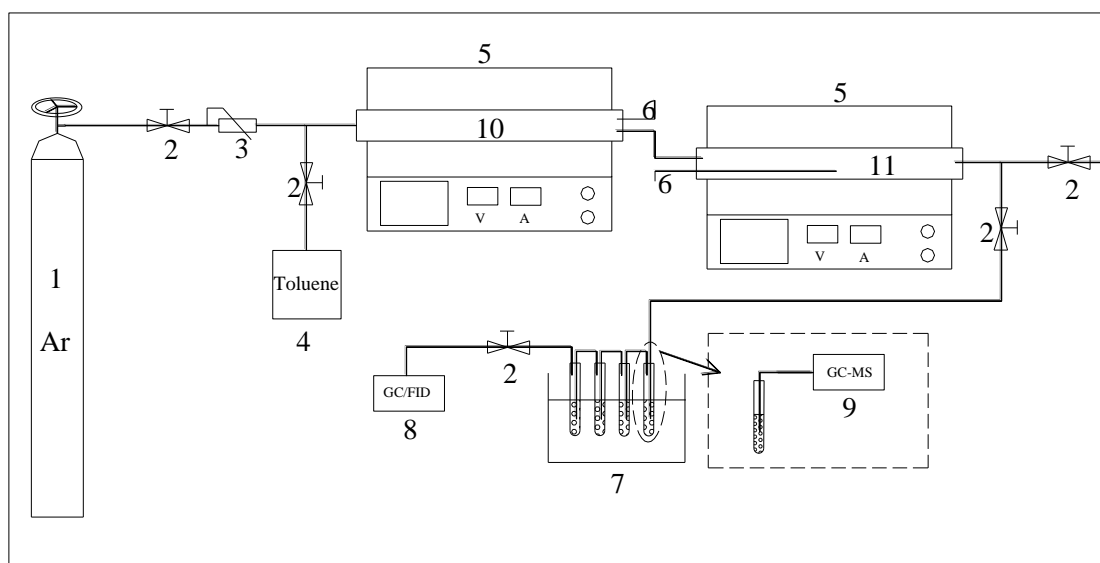


**Fig. 1.** A schematic diagram of the experimental set-up for tar reformation experiments: 1. argon; 2. control valve; 3. gas flow meter; 4. peristaltic pump; 5. electrical furnace; 6. thermocouples; 7. tar condensing unit; 8. GC/TCD and FID; 9. GC/MS; 10. gasification bed; 11. catalytic bed

Argon was used as a carrier gas for the reforming reactor. The argon flow rate was varied in the range of 0.24 to 0.62 L/min to guarantee that the gas residence time remained the same at different reforming temperatures. The gasification temperature was kept at 300 °C to convert toluene into gas. The toluene was fed by a peristaltic pump in the range of 0.29 to 0.70 mL/min (20% toluene concentration) when the gasifier temperature was 300 °C. The volatiles (mostly a mixture of toluene and argon) from gasification went through the reactor and then condensed outside the reactor. The reformation experiments were performed from 650 to 850 °C, and the catalysts were pre-loaded into the catalytic reactor before the reactor was heated. The produced gas including tar passed by the catalyst bed; then, the tarry materials were cracked in the catalyst bed. The amount of catalyst was approximately 3.0 g (15 cm in length) for all experiments conducted in this study, and the gas residence time of the volatiles passing through the catalyst bed was approximately 1 to 2 s. The reactor was lifted out of the furnace and cooled when the experiments finished. Each experiment was done twice.

The gas products were collected from the tar condensing unit for 5 min with a 10-L Tellar sampling bag, and repeatability experiments were performed. All gas products were analyzed online by an Agilent Technologies 7890A gas chromatograph (USA). H<sub>2</sub>, CO, CO<sub>2</sub>, and CH<sub>4</sub> were determined by Thermal Conductivity Detector (TCD) with a molecular sieve and Carboxen columns (Li *et al.* 2013).

The toluene conversion can be defined by Eq. 1,

$$\text{Toluene conversion, } X(\%) = \frac{C_{in} - C_{out}}{C_{in}} \times 100\% \quad (1)$$

where  $C_{in}$  and  $C_{out}$  are the toluene volume flow rate of the inlet and exit components, respectively, in mL/min.

Gas production rate ( $\varphi$ ) was calculated using Eq. 2,

$$\varphi \left( \frac{\text{mL}}{\text{mL}} \right) = \frac{V_{\text{gas (H}_2, \text{CH}_4, \text{CO, CO}_2, \text{ or total gas)}}}{V_{\text{toluene}}} \quad (2)$$

where  $V_{\text{gas (H}_2, \text{CH}_4, \text{CO, CO}_2, \text{ or total gas)}}$  and  $V_{\text{toluene}}$  are the gas flow rate of the exit component and toluene flow rate of the inlet component, respectively, in mL/min.

Gas product composition was calculated using Eq. 3:

$$\begin{aligned} \text{Product comp. } (\%) \\ = \frac{\text{Volume of each gaseous product}}{\text{Total volume of gas products (H}_2 + \text{CO} + \text{CO}_2 + \text{CH}_4)} \times 100\% \end{aligned} \quad (3)$$

### Characterization of Samples

The concentrations of the alkali and alkaline earth metallic (AAEM) species in the samples were quantified by inductively coupled plasma-mass spectroscopy (ICP-MS) (iCAP 6000 series, Thermo Fisher Scientific, USA). The samples were first burned in a muffle furnace as follows: the samples were heated from room temperature to 200 °C at a heating rate of 10 °C /min and maintained for 1.5 h; the temperature was then slowly ramped up to 450 °C and held at 450 °C for 2 h. The ash was digested with HCl and HNO<sub>3</sub> acids (Suprapur, 65%) (volumetric ratio 3:1) until the residue was dissolved. Then, the digestion liquid was diluted 20 times and the dilution liquid was subjected to ICP-MS.

X-ray diffraction (XRD) patterns of the catalysts were scanned by a Bruker D8-Advance (Germany) with Cu K radiation (30 kV and 15 mA) over a  $2\theta$  range from 5 to 90°, with a scanning rate of 3°/min.

The morphology of the catalysts was analyzed by scanning electron microscopy (SEM) using a Hitachi S-4700 (Japan). Magnification of 5000 times was used.

An N<sub>2</sub> adsorption-desorption experiment was performed in a Thermo Scientific Surfer (USA) at 77 K. The specific surface areas and pore volumes were calculated according to the Brunauer-Emmett-Teller (BET) method. The Barrett-Joyner-Halenda (BJH) method was used to derive the mesopore and micropore surface area.

The tar derived from the gasification was captured by four washing bottles serially immersed in cold traps filled with isopropanol (approximately 85 mL). The isopropanol bath was cooled by a refrigerator to maintain a temperature under -18 °C, at which tar and moisture would be completely collected. To ensure the maximum collection of tar, glass beads with a diameter of approximately 3 mm were loaded into the bottles to enlarge the heat transfer area. The tar was considered to be efficiently captured when almost no color was observed in the last washing bottle. When the experiments finished, the solvent in the last bottle was used to wash the outlet of the reactor and other bottles as well as the glass beads. Pure solvent was then used to further wash all bottles and tubes, and, finally, all tar solutions were gathered into a glass vial.

### Tar Characterization by GC – MS

The yields of collected toluene were quantitatively determined by a Thermo Fisher (USA) Trace ISQ chromatography-mass spectrometry (GC-MS) device to calculate the toluene conversion. Isopropanol was chosen as the solvent for tar dissolving. The chromatographic column was a TR-WAXMS capillary column with a size of 30 m × 0.25 mm × 0.25 μm. The column temperature was held at 40 °C for 3 min, and then ramped up to 200 °C at a heating rate of 15 °C/min, lasting 3 min. The ion source in the mass spectrum was electron ionization. The temperatures of the mass spectrum ion source and transmission line were 280 and 250 °C, respectively. The sample was injected by shunting at a split ratio of 1:30, and the temperature of the injection port was 200 °C. The mass spectrum detection started at 4.5 min. The qualitative scanning range was from 35 to 500 amu, and the quantitative scanning range was 65, 91, and 92 amu.

## RESULTS AND DISCUSSION

### Effect of Temperature and Residence Time on Toluene Conversion

Figure 2 shows the effect of temperature on toluene conversion using various catalysts. Ni+bio-char and bio-char+Ni catalysts exhibited excellent catalytic activities in a wide temperature range of 650 to 850 °C with a toluene conversion rate higher than 73%. The catalytic activity of Ni+bio-char catalyst especially became prominent at temperatures higher than 800 °C, at which toluene could be completely converted to small gas molecules with a conversion rate of 99.92%. Although the toluene conversion rate decreased to 96.97% when the temperature was increased above 850 °C, Ni+bio-char catalyst still presented better catalytic activities than those of bio-char+Ni, which had the highest toluene conversion rate of 93.86% at 850 °C. This was in good agreement with the results found by Yue *et al.* (2010), who used a 10 wt% NiO/MgO-Al<sub>2</sub>O<sub>3</sub> catalyst to investigate the

reaction performance of toluene. Although bio-char catalyst showed an increased toluene conversion rate with increasing temperature, the catalytic effect on toluene conversion was inconspicuous within our range of temperatures, and its highest catalytic activities were at 850 °C with a toluene conversion rate of 86.79%. The results indicated that Ni+bio-char had higher catalytic activities than bio-char and bio-char+Ni. Thus, the rank of catalytic activity was Ni+bio-char > bio-char+Ni > bio-char. Overheating usually causes sintering of the catalyst and consumes more energy at temperatures above 800 °C; therefore, 800 °C was considered an appropriate temperature for toluene removal in this study.

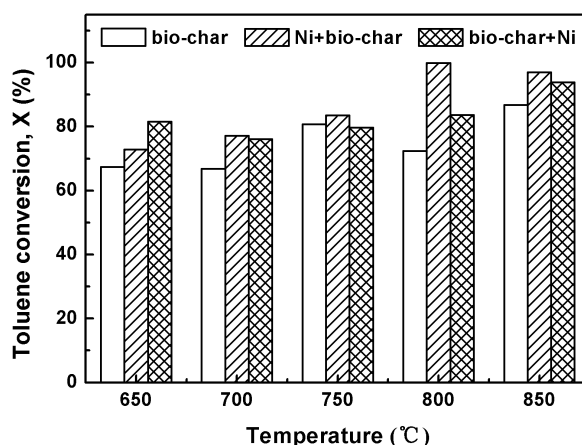


**Fig. 2.** Effect of temperature on toluene conversion for three catalysts at 1.5 s gas residence time

Figure 3 shows the effect of gas residence time on toluene conversion at 800 °C. The influence of gas residence time on toluene conversion differed for the three catalysts. For Ni+bio-char catalyst, the gas residence time had no obvious effect on the toluene conversion at high temperatures because the toluene conversion rate reached 99.90% at such temperatures.

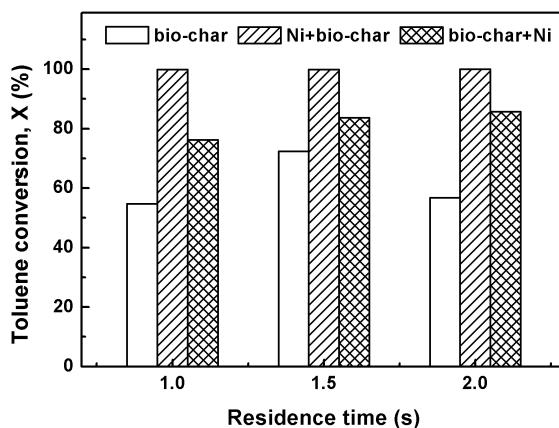


**Fig. 3.** Effect of gas residence time on toluene conversion for three catalysts at 800 °C

The toluene conversion rate of bio-char increased from 54.77% to 72.45% when the gas residence time increased from 1.0 to 1.5 s, and then decreased to 56.70% when the gas residence time increased to 2.0 s. For bio-char+Ni catalyst, the toluene conversion rate increased slightly with increasing gas residence time. It was also found that when the gas residence time increased to more than 1.5 s, the rate of increase of toluene conversion

gradually slowed. Therefore, 1.5 s gas residence time at 800 °C was chosen as the optimal condition in our experiment for economic reasons.

### Effect of Temperature on Gas Compositions

The main compositions, involving the components H<sub>2</sub>, CH<sub>4</sub>, CO, and CO<sub>2</sub> of the final gas product from the tar reformation experiments as a function of temperature for the three catalysts, are shown in Fig. 4. The amount of gas yield increased with increasing temperature for all three catalysts. In particular, the maximum gas yield was 432 mL/(mL C<sub>7</sub>H<sub>8</sub>) for Ni+bio-char catalyst at 850 °C. H<sub>2</sub> was the main gas product over the whole temperature range for all three catalysts. H<sub>2</sub> and CH<sub>4</sub> yields increased with increasing temperature. The yields of H<sub>2</sub> and CH<sub>4</sub> were 339 and 85 mL/(mL C<sub>7</sub>H<sub>8</sub>), 144 and 72 mL/(mL C<sub>7</sub>H<sub>8</sub>), and 233 and 89 mL/(mL C<sub>7</sub>H<sub>8</sub>) using Ni+bio-char, bio-char+Ni and bio-char catalysts, respectively, at 850 °C. These results were attributed to the different structures of the three catalysts. Nickel ions could be evenly dispersed over the catalyst surface to improve the activity of Ni+bio-char catalyst, whereas they could block the pores of bio-char+Ni catalyst.

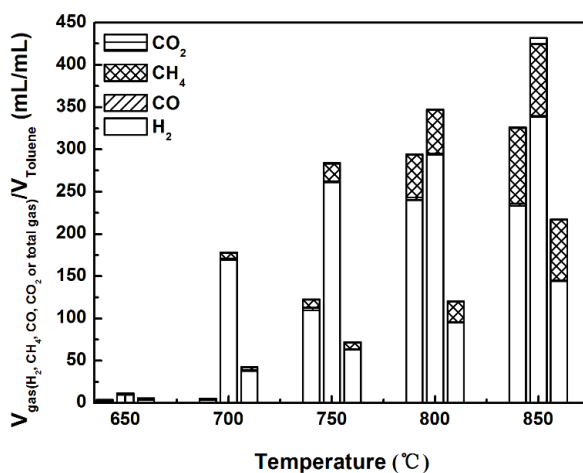


**Fig. 4.** Effect of temperature on gas yield and compositions for three catalysts at 1.5 s gas residence time. The first column is bio-char, the second is Ni+bio-char, and the third is bio-char+Ni.

Many corresponding and sequential reactions can occur in tar reformation reactions, and the product distribution is the result of competition among them (Li *et al.* 2009). The results showed that the gas products contained more H<sub>2</sub> and less CO. H<sub>2</sub> may react with C<sub>7</sub>H<sub>8</sub> to form C<sub>6</sub>H<sub>6</sub> and CH<sub>4</sub> (Eq. 4) and also may be consumed by benzene hydrocracking to form CH<sub>4</sub> when the temperature exceeds 700 °C (Eq. 5). Therefore, CH<sub>4</sub> formation had a significant effect on the amount of toluene conversion (Yue *et al.* 2010). CO<sub>2</sub> may be a product of CO disproportionation (Eq. 6), which is favored at low temperatures. The reactions between toluene and H<sub>2</sub> would occur easily with bio-char or bio-char+Ni catalysts at high temperatures; thus, compared to Ni+bio-char, bio-char and bio-char+Ni catalysts can produce more CH<sub>4</sub> (27.43%, 20.36%, and 33.04% at 850 °C for bio-char, Ni+bio-char, and bio-char+Ni, respectively) and less H<sub>2</sub> content in the end gas products at high temperatures than at low temperatures (Yu *et al.* 2006). Moreover, it is worth noting that Ni+bio-char catalyst showed higher H<sub>2</sub> production than bio-char+Ni catalyst, which may generate a less ordered carbon structure within the biomass char (Zhang *et al.* 2013c).

Hydrodealkylation:



Benzene hydrocracking:



CO disproportionation:



Comparison of gas compositions between Ni+bio-char and bio-char+Ni catalysts indicates that the nickel impregnation method had different effects on gas compositions, although they both led to the increase of toluene conversion, implying that nickel could indeed catalyze  $\text{C}_7\text{H}_8$  to form  $\text{H}_2$  as well as enhance  $\text{C}_6\text{H}_6$  to form  $\text{CH}_4$ , in agreement with previous research results (Yu *et al.* 2007). On the one hand, nickel ions could be evenly dispersed over the catalyst surface to form an “active site”; on the other hand, nickel ions could associate with functional groups ( $-\text{COOH}$ ,  $-\text{OH}$ ) to act as catalysts (Yu *et al.* 2006).

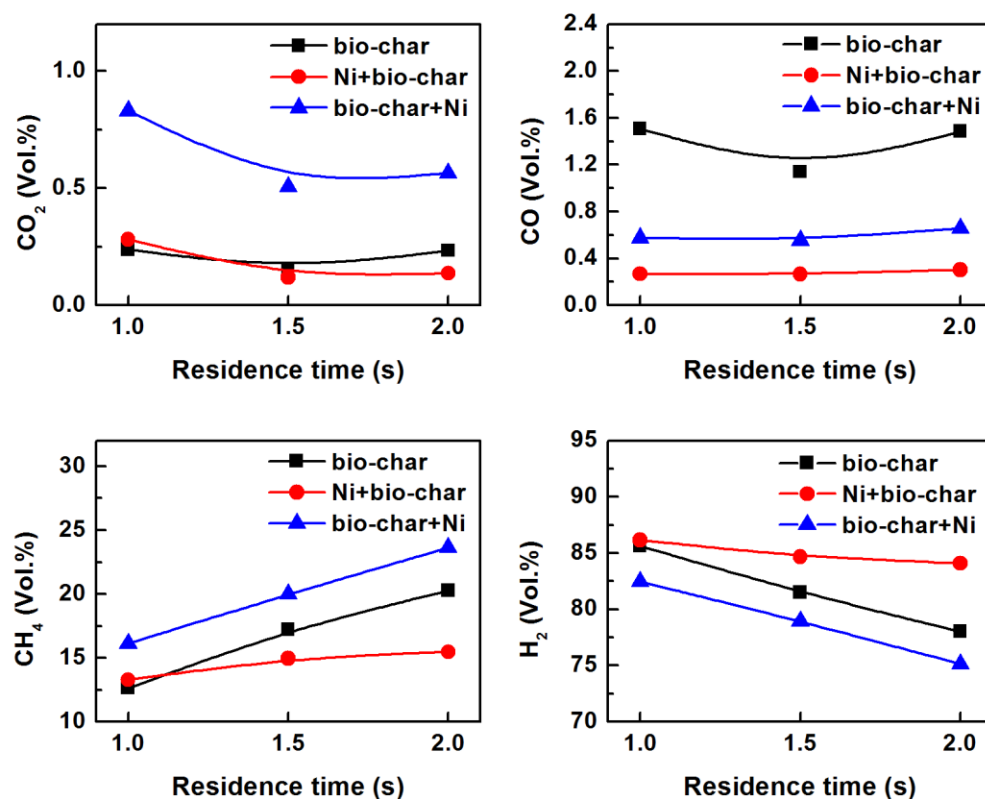


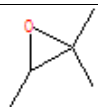
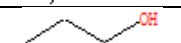
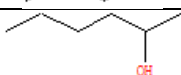
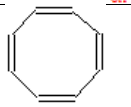
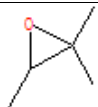
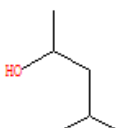
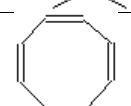
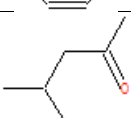
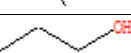
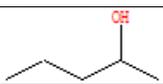
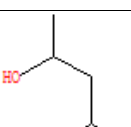
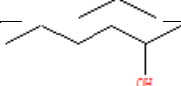
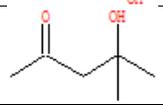
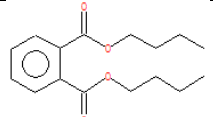
Fig. 5. Effect of gas residence time on gas distribution for three catalysts at 800 °C

Figure 5 shows the main gas components (*e.g.*,  $\text{H}_2$ ,  $\text{CH}_4$ ,  $\text{CO}$ , and  $\text{CO}_2$ ) as a function of gas residence time (1, 1.5, and 2 s) for the three catalysts at 800 °C. As shown in Fig. 5, the gas composition trends were different. For all three catalysts,  $\text{H}_2$  content decreased while  $\text{CH}_4$  content increased with increasing gas residence time.  $\text{CO}$  and  $\text{CO}_2$  contents first decreased and then increased with increasing gas residence time. Compared with bio-char and bio-char+Ni, Ni+bio-char led to more  $\text{H}_2$  content and less  $\text{CO}$ ,  $\text{CO}_2$ , and  $\text{CH}_4$  content at any gas residence time. The product distribution was also regarded as a result of the competition among reactions.

## GC-MS Analysis of Tar

Table 2 compares the GC-MS results of tar using three catalysts at 800 °C.

**Table 2.** Comparison of GC-MS Results for Three Catalysts (a. bio-char, b. Ni+bio-char, c. bio-char+Ni)

	Time	Name of Compound	Chemical Formula	Structure	Molecular Weight
a	4.40	Oxirane,trimethyl-	C <sub>5</sub> H <sub>10</sub> O		86
	4.85	1-Propanol	C <sub>3</sub> H <sub>8</sub> O		60
	6.53	2-Hexanol	C <sub>6</sub> H <sub>14</sub> O		102
	7.70	1,3,5,7-Cyclooctatetrane	C <sub>8</sub> H <sub>8</sub>		108
b	4.42	Oxirane,trimethyl-	C <sub>5</sub> H <sub>10</sub> O		86
	4.86	1-Propanol	C <sub>3</sub> H <sub>8</sub> O		60
	6.54	2-Pentanol,4-methyl-	C <sub>6</sub> H <sub>14</sub> O		102
	7.70	1,3,5,7-Cyclooctatetrane	C <sub>8</sub> H <sub>8</sub>		108
c	4.43	Methyl isobutyl ketone	C <sub>6</sub> H <sub>12</sub> O		100
	4.87	1-Propanol	C <sub>3</sub> H <sub>8</sub> O		60
	5.97	2-Pentanol	C <sub>5</sub> H <sub>12</sub> O		88
	6.18	3-Penten-2-one,4-methyl-	C <sub>6</sub> H <sub>10</sub> O		98
	6.55	2-Pentanol,4-methyl-	C <sub>6</sub> H <sub>14</sub> O		102
	7.2	2-Hexanol	C <sub>6</sub> H <sub>14</sub> O		102
	8.81	2-Pentanol,4-hydroxy-4-methyl-	C <sub>6</sub> H <sub>12</sub> O <sub>2</sub>		116
	16.63	Dibutyl phthalate	C <sub>6</sub> H <sub>22</sub> O <sub>4</sub>		278

The compounds catalyzed by bio-char and Ni+bio-char catalysts were mostly hydrocarbons such as oxirane, trimethyl-, 2-pentanol, 4-methyl-, and 1,3,5,7-cyclooctatetraene. However, the GC-MS analysis of compounds catalyzed by bio-char+Ni catalyst showed the formation of high-molecular weight hydrocarbons, including 2-pentanol, 4-hydroxy-4-methyl- ( $C_6H_{12}O_2$ ), and dibutyl phthalate ( $C_6H_{22}O_4$ ). The results showed that different catalysts preparation method had different reaction mechanisms. The main chemical states of nickel in Ni+bio-char catalyst were nickel oxides (NiO) and metallic Ni ( $Ni^0$ ), while bio-char+Ni catalyst had more  $Ni^{2+}$  inside the char matrix. Initially,  $Ni^{2+}$  species in the aqueous solution were transformed into the relative stable form of  $Ni(H_2O)_6^{2+}$  (Richardson *et al.* 2013), and then were decomposed into the bunsenite (NiO). During the pyrolysis process, more NiO particles embedded in the carbon matrix of poplar wood were reduced into  $Ni^0$  (Shen and Yoshikawa 2014).  $Ni^0$  had the tendency of toluene decomposition, while  $Ni^{2+}$  had the tendency of toluene reformation of substitution reaction. The different nickel forms differ in their catalytic mechanisms (Shen *et al.* 2015). Thus, there was an apparent different composition of condensates from experiments using Ni+bio-char and bio-char +Ni. Bio-char catalyst was a good catalyst and played a key role in toluene reformation, and nickel added into the char can accelerate the toluene reformation process (Shen *et al.* 2015). So, although GC/MS results indicated similar condensates composition from experiments using bio-char and Ni+bio-char, the content of compounds was different (data not shown).

### Catalyst Characterization of Tar Reformation

The contents of AAEM such as Mg, Ca, Fe, and Ni in the samples were determined by ICP-MS. The results are presented in Table 3. As can be seen, the content of Fe, Ca, and Mg in bio-char was higher than that in Ni+bio-char and bio-char+Ni. The Ni content noticeably increased after impregnating the biomass or biomass char with nickel nitrate solution. The Ni content in the Ni+bio-char was almost three times that in the bio-char+Ni. This was a result of the porous surface structure of biomass, whereas the surface of the wood char used in the experiments was smooth and less porous and thus could not provide good conditions for deposition of nickel ions. It seems as if high Ni content provided a better catalytic effect.

**Table 3.** Metal Content of the Three Catalysts

Sample	Content ( $\mu\text{g/g}$ )			
	Mg	Ca	Fe	Ni
Bio-char	2043.88	7375.85	607.56	151.77
Ni+bio-char	1551.46	5678.04	256.93	83579.82
Bio-char+Ni	1524.88	5657.76	467.35	31859.48

Figure 6 illustrates the XRD patterns of the samples. The results showed that Ni+bio-char catalyst had different structures from other catalysts, which showed higher toluene conversion than other catalysts. Compared the spectrograms with Joint Committee of Powder Diffractions Standards (JCPDS) database, the XRD patterns for Ni+bio-char catalyst showed characteristic peaks of metallic nickel ( $Ni^0$ ) at  $2\theta = 44, 51$  and  $76^\circ$ , while no characteristic peaks of  $Ni^0$  were detected for bio-char and bio-char+Ni catalysts. The results also confirmed our previous conclusions that the main chemical states of nickel in Ni+bio-char catalyst were nickel oxides (NiO) and metallic Ni ( $Ni^0$ ), while bio-char+Ni

catalyst had more  $\text{Ni}^{2+}$  inside the char matrix. The diffraction peak intensities of  $\text{Ni}^0$  in Ni+bio-char catalyst were very strong, showing their contents were very high, and also indicating that more amorphous structure were formed and the  $\text{Ni}^0$  particles formed were highly dispersed on the surface of the catalysts.

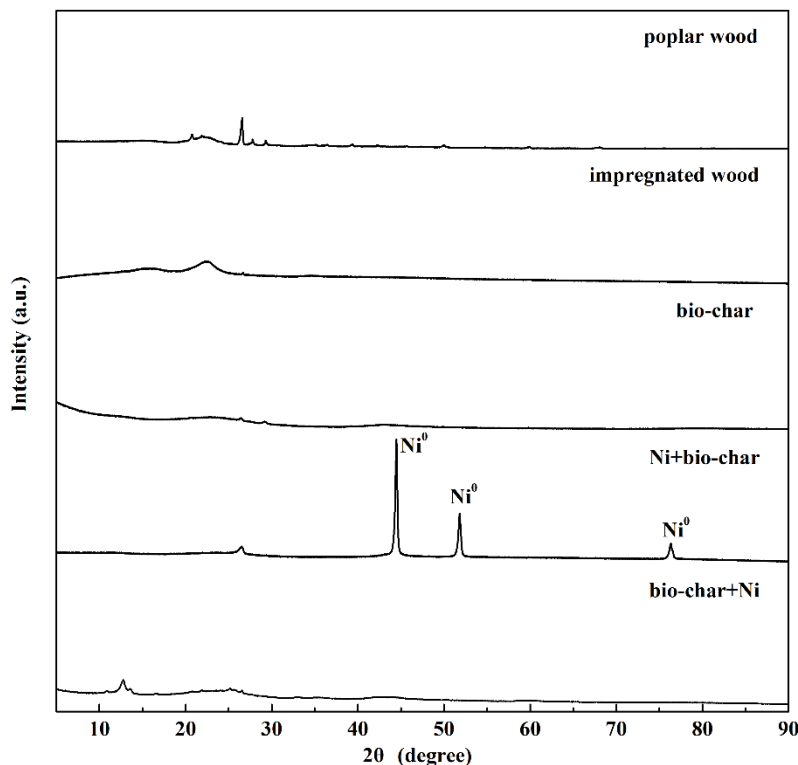


Fig. 6. The XRD patterns of the samples

Generally, the porous structure of solid materials can be divided into three classes recommended by the International Union of Pure and Applied Chemistry (IUPAC): micropores, with a pore size less than 2 nm; mesopores, with a pore diameter between 2 and 50 nm; and macropores larger than 50 nm. The  $\text{N}_2$  adsorption-desorption isotherms of the three catalysts are illustrated in Fig. 7, which provides information about the macropores, mesopores, and micropores. The adsorption isotherms of bio-char belong to a mixture of type III and type IV isotherms with hysteresis loops, which belong to H3 types according to the classification adopted by IUPAC. This indicated the existence of slit-like pores and the presence of macropores and mesopores. For Ni+bio-char catalyst, a steep increase in nitrogen quantity adsorbed at the beginning of the adsorption isotherms implied a mixture of type I and type IV with hysteresis loops and demonstrated the existence of micropores and mesopores.

According to IUPAC, the observed hysteresis loops were a combination of H3 and H4 types, which suggests the existence of slit-like and needle-like pores. The adsorption isotherms of bio-char+Ni belonged to type III, indicating that the catalyst comprised a mostly mesoporous structure. The amount of adsorbed nitrogen is indicative of the adsorptive capacity of the catalysts (Fu *et al.* 2012). It was obvious that, compared to the other two types of catalysts, the adsorption capacity of Ni+bio-char had achieved a huge increase.

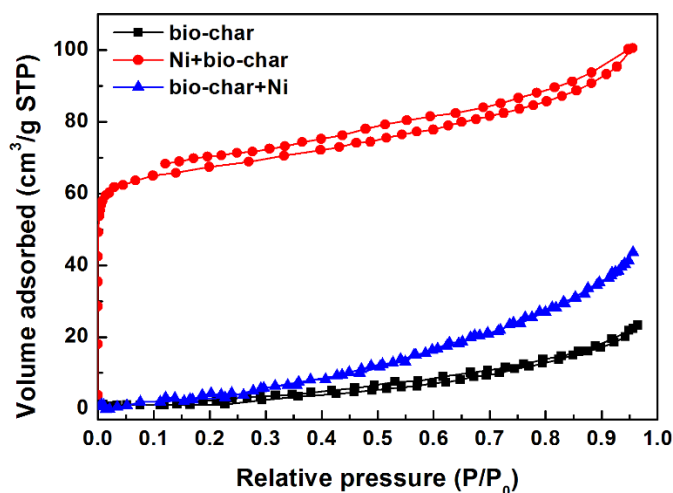


Fig. 7. The N<sub>2</sub> adsorption-desorption curves of the three catalysts

The structural heterogeneity of the porous texture of catalysts is generally characterized by its pore size distribution. Figure 8 presents the pore size distribution of the three catalysts. It is clear that there was a remarkable difference in pore size for the three catalysts. For bio-char, the pore distribution was relatively concentrated, with primarily 35- and 50-nm pores. For Ni+bio-char, the pore distribution was more concentrated and mostly consisted of 36-nm mesopores, which resulted in higher specific surface area, as shown in Table 4. The pore size distribution of bio-char+Ni catalyst was scattered, and more macropores were observed.

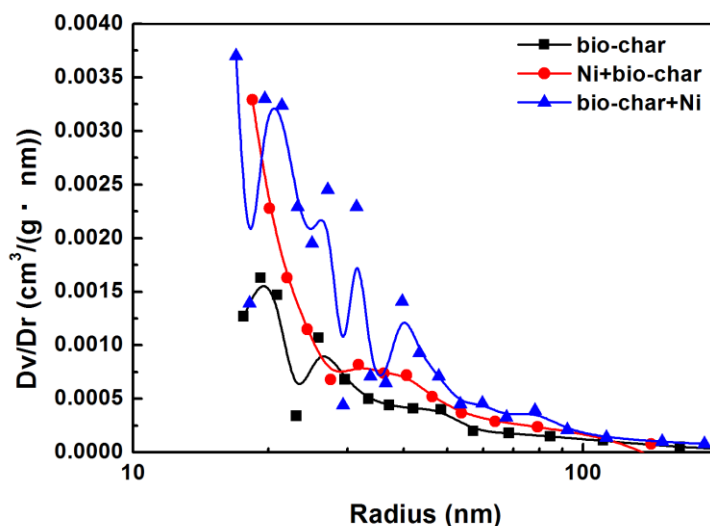


Fig. 8. Pore distribution of three catalysts

Catalytic activity could be influenced by pore volume and specific surface area of a catalyst, which play important roles in tar reformation experiments. The specific surface area and pore volume are appropriate factors for evaluating a catalyst because coke produced from tar reformation would block the pores and reduce the specific surface area (Abu El-Rub *et al.* 2004). Table 4 illustrates the specific surface area and pore volume of the three catalysts in this study. The specific surface area and pore volume of Ni+bio-char

and bio-char+Ni catalysts both increased to some extent. This was especially the case for Ni+bio-char catalyst, which led to the highest toluene conversion (see above) in the present experiments; its specific surface area was 32.87 times that of bio-char and 8.39 times that of bio-char+Ni, indicating that Ni+bio-char was much better than bio-char+Ni and bio-char as a tar-reforming catalyst. The results also indicated that Ni was more easily distributed in biomass than in bio-char.

**Table 4.** BET Surface Area of the Three Catalysts

Materials	Specific surface area (m <sup>2</sup> /g)	Pore volume (cm <sup>3</sup> /g)	Maximum radius (nm)
Bio-char	6.45	1.48	19.23
Ni+bio-char	212.02	48.73	18.42
Bio-char+Ni	25.27	5.81	16.95

The morphologies of bio-char, Ni+bio-char, and bio-char+Ni were examined by SEM, as shown in Fig. 9. It was found that, compared to bio-char and bio-char+Ni catalysts, more porous structures were obtained in Ni+bio-char catalyst, which meant that the adsorption capacity was elevated and the number of active sites was increased. The greater number of pores gave rise to more sufficient cracking/reformation of the tar.

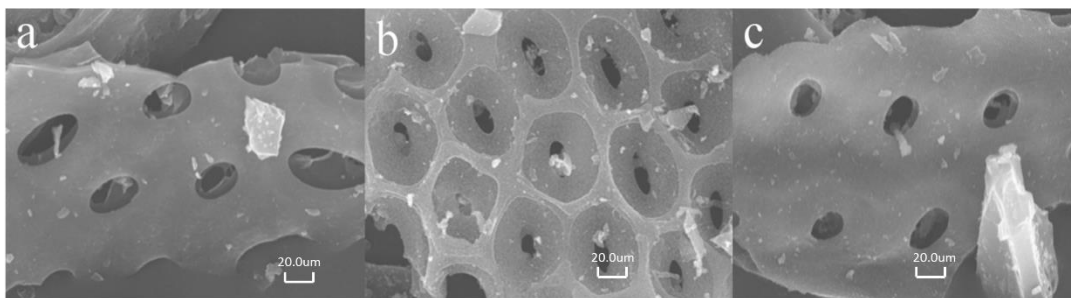


**Fig. 9.** SEM images (5000×) of the three catalysts (a, bio-char; b, Ni+bio-char; c, bio-char+Ni)

## CONCLUSIONS

1. Three types of catalysts (bio-char, Ni+bio-char, and bio-char+Ni) were applied to a catalytic tar reformation model compound. Ni+bio-char catalyst exhibited excellent catalytic activities in a wide temperature range of 650 to 850 °C, especially at 800 °C, where the toluene conversion rate was 99.92%.
2. The gas yield increased with temperature with each of the catalysts, reaching 432 mL/(mL C<sub>7</sub>H<sub>8</sub>) for Ni+bio-char catalyst at 850 °C. In particular, the H<sub>2</sub> and CH<sub>4</sub> yields were 339 and 85 mL/(mL C<sub>7</sub>H<sub>8</sub>) at 850 °C.
3. Ni+bio-char catalyst had better catalytic activities than the other catalysts because toluene could be completely converted to small gas molecules and the specific surface area of Ni+bio-char catalyst was 32.87 and 8.39 times that of bio-char and bio-char+Ni catalysts, respectively. Moreover, metallic nickel (Ni<sup>0</sup>) particles could be generated in the carbon matrix of Ni+bio-char catalyst *via* pyrolysis.

4. Tar and char are always unwanted byproducts of the gasification process. The new concept of catalyst use presented in this work provides a sustainable method to simultaneously process these waste byproducts and convert them into clean energy.

## ACKNOWLEDGMENTS

This research was supported by the National Hi-tech R&D Program of China (863 Program, 2012AA101809).

## REFERENCES CITED

- Abu El-Rub, Z., Bramer, E. A., and Brem, G. (2004). "Review of catalysts for tar elimination in biomass gasification processes," *Ind. Eng. Chem. Res.* 43(22), 6911-6919. DOI: 10.1021/ie0498403
- Donahue, C. J., and Rais, E. A. (2009). "Proximate analysis of coal," *J. Chem. Educ.* 86(2), 222. DOI: 10.1021/ed086p222
- Fu, P., Hu, S., Xiang, J., Yi, W., Bai, X., Sun, L., and Su, S. (2012). "Evolution of char structure during steam gasification of the chars produced from rapid pyrolysis of rice husk," *Bioresour. Technol.* 114, 691-697. DOI: 10.1016/j.biortech.2012.03.072.
- Furusawa, T., and Tsutsumi, A. (2005). "Development of cobalt catalysts for the steam reforming of naphthalene as a model compound of tar derived from biomass gasification," *Appl. Catal. A-Gen.* 278(2), 195-205. DOI: 10.1016/j.apcata.2004.09.034.
- Han, J., and Kim, H. (2008). "The reduction and control technology of tar during biomass gasification/pyrolysis: An overview," *Renew. Sust. Energ. Rev.* 12(2), 397-416. DOI: 10.1016/j.rser.2006.07.015.
- Kong, M., Fei, J. H., Wang, S. A., Lu, W., and Zheng, X. M. (2011). "Influence of supports on catalytic behavior of nickel catalysts in carbon dioxide reforming of toluene as a model compound of tar from biomass gasification," *Bioresour. Technol.* 102(2), 2004-2008. DOI: 10.1016/j.biortech.2010.09.054.
- Le, D. D., Xiao, X., Morishita, K., and Takarada, T. (2009). "Biomass gasification using nickel loaded brown coal char in fluidized bed gasifier at relatively low temperature," *J. Chem. Eng. Jpn.* 42(1), 51-57. DOI: 10.1252/jcej.08we218.
- Lee, I. G., and Ihm, S. K. (2009). "Catalytic gasification of glucose over Ni/activated charcoal in supercritical water," *Ind. Eng. Chem. Res.* 48(3), 1435-1442. DOI: 10.1021/ie8012456.
- Li, C., and Suzuki, K. (2009). "Tar property, analysis, reforming mechanism and model for biomass gasification-an overview," *Renew. Sust. Energ. Rev.* 13(3), 594-604. DOI: 10.1016/j.rser.2008.01.009.
- Li, C., Hirabayashi, D., and Suzuki, K. (2009). "Development of new nickel based catalyst for biomass tar steam reforming producing H<sub>2</sub>-rich syngas," *Fuel Process. Technol.* 90(6), 790-796. DOI: 10.1016/j.fuproc.2009.02.007.
- Li, Y. Q., Zhang, R. H., Liu, X. Y., Chen, C., Xiao, X., Feng, L., He, Y. F., and Liu, G. Q. (2013). "Evaluating methane production from anaerobic mono- and codigestion of kitchen waste, corn stover, and chicken manure," *Energ. Fuel.* 27, 2085-2091. DOI: 10.1021/ef400117f.

- Min, Z., Asadullah, M., Yimsiri, P., Zhang, S., Wu, H., and Li, C-Z (2011a). "Catalytic reforming of tar during gasification. Part I. Steam reforming of biomass tar using ilmenite as a catalyst," *Fuel* 90(5), 1847-1854. DOI: 10.1016/j.fuel.2010.12.039.
- Min, Z. H., Yimsiri, P., Asadullah, M., Zhang, S., and Li, C. Z. (2011b). "Catalytic reforming of tar during gasification. Part II. Char as a catalyst or as a catalyst support for tar reforming," *Fuel* 90(7), 2545-2552. DOI: 10.1016/j.fuel.2011.03.027
- Park, H. J., Park, S. H., Sohn, J. M., Park, J., Jeon, J. K., Kim, S. S., and Park, Y. K. (2010). "Steam reforming of biomass gasification tar using benzene as a model compound over various Ni supported metal oxide catalysts," *Bioresour. Technol.* 101, S101-S103. DOI: 10.1016/j.biortech.2009.03.036.
- Richardson, Y., Motuzas, J., Julbe, A., Volle, G., and Blin, J. (2013). "Catalytic investigation of *in situ* generated ni metal nanoparticles for tar conversion during biomass pyrolysis," *Journal of Physical Chemistry C*, 117(45), 23812-23831. DOI: 10.1021/jp408191p.
- Sato, K., and Fujimoto, K. (2007). "Development of new nickel based catalyst for tar reforming with superior resistance to sulfur poisoning and coking in biomass gasification," *Catal. Commun.* 8(11), 1697-1701. DOI: 10.1016/j.catcom.2007.01.028.
- Shen, Y. F., Chen, M. D., Sun, T. H., and Jia, J. P. (2015). "Catalytic reforming of pyrolysis tar over metallic nickel nanoparticles embedded in pyrochar," *Fuel* 159, 570-579. DOI: 10.1016/j.fuel.2015.07.007.
- Shen, Y. F., and Yoshikawa, K. (2014). "Tar conversion and vapor upgrading via *in situ* catalysis using silica-based nickel nanoparticles embedded in rice husk char for biomass pyrolysis/gasification" *Industrial & Engineering Chemistry Research* 53(27), 10929-10942. DOI: 10.1021/ie501843y.
- Shen, Y., Zhao, P., Shao, Q., Takahashi, F., and Yoshikawa, K. (2014). "*In situ* catalytic conversion of tar using rice husk char/ash supported nickel-iron catalysts for biomass pyrolytic gasification combined with the mixing-simulation in fluidized-bed gasifier," *Appl. Energ.* DOI: 10.1016/j.apenergy.2014.10.074.
- Swierczynski, D., Courson, C., and Kiennemann, A. (2008). "Study of steam reforming of toluene used as model compound of tar produced by biomass gasification," *Chem. Eng. Process.* 47(3), 508-513. DOI: 10.1016/j.cep.2007.01.012.
- Wang, D. (2013). "Study of Ni/char catalyst for biomass gasification in an updraft gasifier: Influence of catalyst granular size on catalytic performance," *BioResources* 8(3), 3479-3489. DOI: 10.15376/biores.8.3.3479-3489
- Wang, D., Yuan, W., and Ji, W. (2010). "Use of biomass hydrothermal conversion char as the ni catalyst support in benzene and gasification tar removal," *T. ASAE.* 53(3), 795-800.
- Wang, D., Yuan, W. Q., and Ji, W. (2011). "Char and char-supported nickel catalysts for secondary syngas cleanup and conditioning," *Appl. Energ.* 88(5), 1656-1663. DOI: 10.1016/j.apenergy.2010.11.041.
- Xu, C. C., Donald, J., Byambajav, E., and Ohtsuka, Y. (2010). "Recent advances in catalysts for hot-gas removal of tar and NH<sub>3</sub> from biomass gasification," *Fuel* 89(8), 1784-1795. DOI: 10.1016/j.fuel.2010.02.014.
- Yu, J., Tian, F.-J., and Li, C.-Z. (2007). "Novel water-gas-shift reaction catalyst from iron-loaded Victorian brown coal," *Energ. Fuel.* 21(2), 395-398. DOI: 10.1016/j.fuel.2010.02.014.

- Yu, J. L., Tian, F. J., Chow, M. C., McKenzie, L. J., and Li, C. Z. (2006). "Effect of iron on the gasification of Victorian brown coal with steam: enhancement of hydrogen production," *Fuel* 85(2), 127-133. DOI: 10.1016/j.fuel.2005.05.026.
- Yue, B., Wang, X., Ai, X., Yang, J., Li, L., Lu, X., and Ding, W. (2010). "Catalytic reforming of model tar compounds from hot coke oven gas with low steam/carbon ratio over Ni/MgO-Al<sub>2</sub>O<sub>3</sub> catalysts," *Fuel Process. Technol.* 91(9), 1098-1104. DOI: 10.1016/j.fuproc.2010.03.020.
- Yung, M. M., Jablonski, W. S., and Magrini-Bair, K. A. (2009). "Review of catalytic conditioning of biomass-derived syngas," *Energ. Fuel.* 23, 1874-1887. DOI: 10.1021/ef800830n.
- Zhang, C. Y. (2013a). "Study on pyrolysis and its reaction kinetics of agricultural and forestry biomass," Master Dissertation, Beijing University of Chemical Technology, Beijing, China.
- Zhang, L., Matsuhara, T., Kudo, S., Hayashi, J., and Norinaga, K. (2013b). "Rapid pyrolysis of brown coal in a drop-tube reactor with co-feeding of char as a promoter of in situ tar reforming," *Fuel* 112, 681-686. DOI: 10.1016/j.fuel.2011.12.030.
- Zhang, S., Asadullah, M., Dong, L., Tay, H.-L., and Li, C.-Z. (2013c). "An advanced biomass gasification technology with integrated catalytic hot gas cleaning. Part II: Tar reforming using char as a catalyst or as a catalyst support," *Fuel* 112, 646-653. DOI: 10.1016/j.fuel.2013.03.015.
- Zhao, B., Zhang, X., Chen, L., Qu, R., Meng, G., Yi, X., and Sun, L. (2010). "Steam reforming of toluene as model compound of biomass pyrolysis tar for hydrogen," *Biomass Bioenerg.* 34(1), 140-144. DOI: 10.1016/j.biombioe.2009.10.011.

Article submitted: September 16, 2015; Peer review completed: November 23, 2015;  
Revised version received and accepted: February 4, 2016; Published: March 7, 2016.  
DOI: 10.15376/biores.11.2.3752-3768